Citation information: DOI: 10.1109/jiot.2026.3660101, IEEE Internet of Things Journal

Regional Control Subject to Actuator Amplitude and Rate Constraints Under Communication Protocols

Yonggang Chen, Zidong Wang, Juan Wang and Lan Lan

***Abstract*—This paper addresses the regional control problem for networked systems under simultaneous actuator amplitude and rate constraints. Communication protocols are employed to manage signal transmission over the constrained network. Under the round-robin and try-once-discard protocols, sufficient conditions are derived, expressed as nonlinear matrix inequalities, to ensure the boundedness, H_∞ performance, and asymptotic stability of the closed-loop systems. Some algorithms are proposed to optimize the performance indices under linear matrix inequality constraints. Two numerical examples illustrate the validity of the obtained results. Unlike earlier studies that focus mainly on communication protocols or amplitude constraints alone, this paper explicitly incorporates actuator rate constraints and systematically designs static feedback gains rather than assuming them known. As a result, the proposed method yields a less conservative estimate of the domain of attraction even under amplitude-only constraints, while maintaining simpler controller implementation compared to dynamic output-feedback strategies.**

***Index Terms*—Regional control, networked systems, actuator constraints, amplitude and rate constraints, communication protocols.**

I. Introduction

In reality, almost all physical actuators are subject to amplitude constraints, which may lead to performance degradation, multiple equilibria, and instability in closed-loop systems [23], [40]. Over the past several decades, the analysis and synthesis of control systems with amplitude-saturating actuators have been extensively studied, and numerous significant results have been established (see, e.g., [2], [3], [18], [22], [27], [48], [51], [56], [57] and the references therein). In the context of regional (local) control, prevalent methods for handling saturation nonlinearities include the polytopic model representations [23], [57] and the generalized sector condition [3], [40].

This work was supported in part by the National Natural Science Foundation of China under Grant 62273132, in part by the Natural Science Foundation of Henan Province of China under Grant 242300421052, in part by the Royal Society of the UK, and in part by the Alexander von Humboldt Foundation of Germany. (*Corresponding author: Juan Wang*).

Yonggang Chen is with the School of Mathematics and Statistics, Xinyang Normal University, Xinyang 464000, China, and also with the School of Mathematical Sciences, Henan Institute of Science and Technology, Xinxiang 453003, China (e-mail: happycygzmd@163.com).

Juan Wang and Lan Lan are with the School of Mathematics and Statistics, Xinyang Normal University, Xinyang 464000, China (e-mails: dotey99@126.com; lanmath@126.com).

Zidong Wang is with the Department of Computer Science, Brunel University of London, Uxbridge UB8 3PH, U.K. (e-mail: Zidong.Wang@brunel.ac.uk).

In some real-world control systems, such as flight control systems [21], industrial processes [46], wind turbine systems [14], and power systems [24], actuator rate constraints are also inevitable, which can further degrade system performance and even lead to instability. As a result, over the past two decades, many researchers have concentrated on actuator-saturated systems with both amplitude and rate constraints [9], [16], [17], [25], [28], [33], [34], [54]. For instance, in [16], the regional feedback stabilization problem has been addressed by utilizing first-order models to represent both amplitude and rate constraints. Following the same actuator models as in [16], the stability and stabilization problems have been investigated in [34] under a sampled-data based control scheme.

On the other hand, networked control systems (NCSs) have attracted significant research attention over the past two decades due to their notable advantages and widespread applications [19], [31]. However, network-induced challenges, such as packet dropouts, transmission delays, and data quantization, are unavoidable primarily because of bandwidth constraints [1], [52]. To reduce communication resource usage, event-triggered data transmission mechanisms have been proposed, and various analysis and synthesis criteria have been derived for NCSs [5], [8], [15], [35]–[37], [41], [53]. Furthermore, communication protocols have been integrated into NCSs to prevent data collisions caused by bandwidth limitations and to support multiple packet transmissions [13], [20], [26], [29], [42], [45], [49], [55], [58]. Common communication protocols used in some specific industrial applications include the random access (RA) protocol, round-robin (RR) protocol, and try-once-discard (TOD) protocol.

Considering actuator constraints, several pioneering analysis and design criteria have been developed for NCSs over the past decade [4], [6], [10], [30], [32], [43], [47], [50]. For instance, the emulation and co-design problems have been addressed in [6] for LPV systems with input saturations under two event-triggering conditions. Using a time-delay approach, the stability analysis has been carried out in [30] for NCSs with control constraints under the RR and TOD protocols, respectively. In [4], a dynamic output-feedback controller has been designed via a switched model for actuator-saturated state-delayed systems under the RR protocol. However, it should be noted that these works primarily address control amplitude constraints, whereas *rate constraints* of actuators have received little attention apart from [10], in which a robust event-triggered data-driven control scheme has been proposed under both control amplitude and rate constraints.

In this paper, the focus is primarily on the regional control problem for NCSs subject to actuator amplitude and rate

constraints under the RR and TOD protocols, respectively. A dynamic equation with saturated input is first introduced to generate control signals while accounting for both amplitude and rate constraints. Then, by employing switched models to represent actual measurements and utilizing modified sector conditions to address nonlinearities, two sufficient conditions are proposed to ensure the boundedness, H_∞ performance, and asymptotic stability of the closed-loop systems. Furthermore, algorithms are provided to solve the feedback gains with optimized performance. Finally, two numerical examples are presented to show the effectiveness of the proposed results.

The contributions of this paper are summarized as follows. 1) For the first time, the regional control problem for NCSs subject to both amplitude and rate constraints of actuators under communication protocols is addressed, with two sufficient conditions derived through nonlinear matrix inequalities. 2) Iterative algorithms subject to linear matrix inequality (LMI) constraints are proposed to compute the feedback gains with optimized performance. These algorithms eliminate the need for complex and conservative linearization techniques.

Notations. $\mathbb{R}^n$ represents the n-dimensional Euclidean space. $P > 0$ (≥ 0) indicates that P is a symmetric and positive definite (positive semi-definite) matrix. $G_{(i)}$ refers to the i-th row of the matrix G. $u_{(i)}$ denotes the i-th element of the vector u. I is an identity matrix. $\mathbb{I}[a,b] \triangleq \{a, a+1, \ldots, b\}$.

II. Problem formulation

Consider the following linear control system:

$$\begin{cases} x_{k+1} = Ax_k + B\bar{u}_k + Dw_k, \\ y_k = Cx_k + Ew_k,\ z_k = Fx_k \end{cases} \tag{1}$$

where $x_k \in \mathbb{R}^{n_x}$ is the system state, $\bar{u}_k \in \mathbb{R}^{n_u}$ is the control input, $y_k \in \mathbb{R}^{n_y}$ is the measurement output, $z_k \in \mathbb{R}^{n_z}$ is the controlled output, $w_k \in \mathbb{R}^{n_w}$ is the disturbance input, A, B, C, D, E and F are known real constant matrices. The disturbance w_k is assumed to satisfy the energy-bounded condition

$$\sum_{k=0}^{+\infty} w_k^T w_k \leq \mu,\ \mu > 0. \tag{2}$$

Moreover, the actuators are subject to amplitude and rate saturation constraints. The corresponding saturation functions are defined as follows:

$$\begin{aligned} \mathrm{sat}_a(u_{(i)}) &= \mathrm{sign}(u_{(i)})\min\{\hat{u}_{a(i)}, |u_{(i)}|\},\ i \in \mathbb{I}[1, n_u], \\ \mathrm{sat}_r(v_{(i)}) &= \mathrm{sign}(v_{(i)})\min\{\hat{u}_{r(i)}, |v_{(i)}|\},\ i \in \mathbb{I}[1, n_u] \end{aligned}$$

where $\hat{u}_{a(i)}$ and $\hat{u}_{r(i)}$ refer to, respectively, the amplitude saturation level and the rate saturation level.

To represent the actuator saturation constraints, the following dynamic equation can be considered [17]:

$$u_{k+1} = u_k + \mathrm{sat}_r(v_k) \tag{3}$$

where $u_k \in \mathbb{R}^{n_u}$ is the state vector, and $v_k \in \mathbb{R}^{n_u}$ is the feedback input. The actual control input $\bar{u}_k$ is then given by

$$\bar{u}_k \triangleq \mathrm{sat}_a(u_k). \tag{4}$$

Noting the well-known fact as follows:

$$\begin{aligned} \Delta\bar{u}_{k(i)} \triangleq\ & |\bar{u}_{k+1(i)} - \bar{u}_{k(i)}| \\ =& |\mathrm{sat}_a(u_{k(i)} + \mathrm{sat}_r(v_{k(i)})) - \mathrm{sat}_a(u_{k(i)})| \\ \leq& |\mathrm{sat}_r(v_{k(i)})| \leq |\hat{u}_{r(i)}|,\ i \in \mathbb{I}[1, n_u], \end{aligned} \tag{5}$$

it can be observed that $\bar{u}_k$ respects the rate constraints.

Remark 1: In addition to the actuator model described by (3) and (4), an alternative model can be expressed as [33]

$$\bar{u}_{k+1(i)} = \bar{u}_{k(i)} + \mathrm{sat}_r(\lambda_{(i)}(-\bar{u}_{k(i)} + \mathrm{sat}_a(v_{k(i)})))$$

where $\lambda_{(i)} > 0$ ($i \in \mathbb{I}[1, n_u]$) are scalars. This representation is the discrete-time counterpart of the position-feedback-type model [16]. It should be noted, however, that if the actual actuator dynamics deviate from a first-order behavior, this model may not guarantee the closed-loop stability.

In this paper, we consider the scenario where measurements are transmitted through a communication network with limited bandwidth. Under these conditions, data collisions are almost inevitable during transmission, leading to undesired network-induced phenomena such as packet dropouts, packet disorders, and time delays. To mitigate these issues, the RR and TOD communication protocols are employed, where only one sensor node is permitted to transmit data at each instant [29], [58].

Let s be the number of sensors and $y_{j,k} \in \mathbb{R}^{q_j}$ be the measurement from the j-th sensor ($\Sigma_{j=1}^{s} q_j = n_y$). The overall measurement y_k can then be expressed as

$$y_k = \mathrm{col}\{y_{1,k}, y_{2,k}, \ldots, y_{s,k}\}. \tag{6}$$

To model the measurement y_k under the RR and TOD communication protocols, we introduce a function $\sigma_k \in \mathbb{I}[1, s]$ whose value denotes the activated node at the time step k. Then, the actual measurements $\bar{y}_{j,k}$ for each sensor $j \in \mathbb{I}[1, s]$ can be represented as follows [58]:

$$\bar{y}_{j,k} = \begin{cases} y_{j,k},\ j = \sigma_k, \\ \bar{y}_{j,k-1},\ \text{otherwise}. \end{cases} \tag{7}$$

Let us introduce the block diagonal matrix

$$\Psi_{\sigma_k} \triangleq \mathrm{diag}\{\delta(\sigma_k - 1)I, \delta(\sigma_k - 2)I, \ldots, \delta(\sigma_k - s)I\}$$

where $\delta(\cdot)$ is the Kronecker delta function. Furthermore, the actually received measurement can be rewritten as

$$\bar{y}_k = \Psi_{\sigma_k} y_k + (I - \Psi_{\sigma_k})\bar{y}_{k-1}. \tag{8}$$

This paper focuses on designing the feedback input

$$v_k = K_{\sigma_k}^y \bar{y}_k + K_{\sigma_k}^u u_k \tag{9}$$

where K_j^y and K_j^u ($j \in \mathbb{I}[1, s]$) are gain matrices.

The block diagram of the considered control system, subject to actuator amplitude and rate constraints as well as the communication protocol, is presented in Fig. 1.

Define the augmented vector as $\eta_k \triangleq \mathrm{col}\{x_k, u_k, \bar{y}_{k-1}\} \in \mathbb{R}^n$ ($n = n_x + n_u + n_y$) and introduce the nonlinearities

$$\psi_a(u_k) \triangleq \mathrm{sat}_a(u_k) - u_k,\ \psi_r(v_k) \triangleq \mathrm{sat}_r(v_k) - v_k.$$

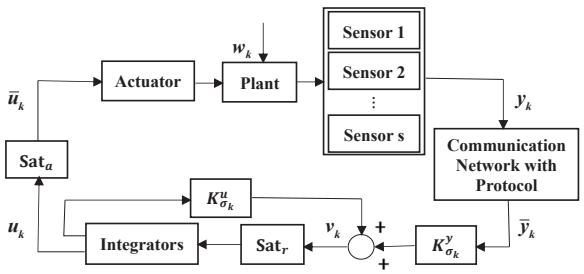

Fig. 1: The block diagram of the control system.

Then, using the equations (1), (3), (4), (8) and (9), the following augmented closed-loop system can be derived:

$$\begin{cases} \eta_{k+1} = (\bar{A}_{\sigma_k} + \mathcal{R}K^y_{\sigma_k}\bar{C}_{\sigma_k} + \mathcal{R}K^u_{\sigma_k}\mathcal{R}^T)\eta_k \\ \qquad +\bar{B}\psi_a(u_k) + \mathcal{R}\psi_r(v_k) \\ \qquad +(\bar{D}_{\sigma_k} + \mathcal{R}K^y_{\sigma_k}\Psi_{\sigma_k}E)w_k, \\ z_k = \bar{F}\eta_k \end{cases} \tag{10}$$

where

$$\bar{A}_{\sigma_k} \triangleq \begin{bmatrix} A & B & 0 \\ 0 & I & 0 \\ \Psi_{\sigma_k}C & 0 & I-\Psi_{\sigma_k} \end{bmatrix},\ \bar{B} \triangleq \begin{bmatrix} B \\ 0 \\ 0 \end{bmatrix},$$
$$\bar{C}_{\sigma_k} \triangleq \begin{bmatrix} \Psi_{\sigma_k}C & 0 & I-\Psi_{\sigma_k} \end{bmatrix},$$
$$\bar{D}_{\sigma_k} \triangleq \begin{bmatrix} D \\ 0 \\ \Psi_{\sigma_k}E \end{bmatrix},\ \mathcal{R} \triangleq \begin{bmatrix} 0 \\ I \\ 0 \end{bmatrix},\ \bar{F} \triangleq \begin{bmatrix} F & 0 & 0 \end{bmatrix}.$$

The initial condition of the system (10) is denoted as $\eta_0 \triangleq \mathrm{col}\{x_0, u_0, \bar{y}_{-1}\}$. In this paper, it is assumed that $\bar{y}_{-1} = 0$. Moreover, the estimate of the domain of attraction (DOA) is characterized by the following ellipsoid:

$$\mathscr{W} \triangleq \{\eta_0 \in \mathbb{R}^n : \eta_0^T\mathcal{P}\eta_0 \le 1,\ \mathcal{P} > 0\}. \tag{11}$$

To handle the saturation-induced nonlinear terms $\psi_a(u_k)$ and $\psi_r(v_k)$, we first recall the following lemma.

Lemma 1: [3], [40] Let $\mathbf{u}, \mathbf{w} \in \mathbb{R}^{n_u}$ be given, and define $\psi(\mathbf{u}) \triangleq \mathrm{sat}(\mathbf{u}) - \mathbf{u}$, where $\mathrm{sat}(\mathbf{u})$ is the saturation function with levels $\hat{\mathbf{u}}_{(i)}$ $(i \in \mathbb{I}[1, n_u])$. Consider the set

$$\mathcal{S}(\mathbf{w}, \hat{\mathbf{u}}) \triangleq \{\mathbf{w} \in \mathbb{R}^{n_u} : |\mathbf{w}_{(i)}| \le \hat{\mathbf{u}}_{(i)}, i \in \mathbb{I}[1, n_u]\}.$$

If $\mathbf{w} \in \mathcal{S}(\mathbf{w}, \hat{\mathbf{u}})$, then for any $n_c \times n_c$ diagonal matrix $H > 0$,

$$\psi^T(\mathbf{u})H[\psi(\mathbf{u}) + \mathbf{u} - \mathbf{w}] \le 0.$$

For given $n_u \times n$ matrices G^a_j and G^r_j $(j \in \mathbb{I}[1, s])$, take the vector $\mathbf{w}$ in Lemma 1 as $\mathbf{w} = G^a_j\eta$ and $\mathbf{w} = G^r_j\eta$, respectively. Then, we can define the following polyhedral sets:

$$\mathcal{S}(G^a_j, \hat{u}_a) \triangleq \{\eta \in \mathbb{R}^n : |G^a_{j(i)}\eta| \le \hat{u}_{a(i)}, \\ i \in \mathbb{I}[1, n_u]\},\ j \in \mathbb{I}[1, s], \tag{12}$$
$$\mathcal{S}(G^r_j, \hat{u}_r) \triangleq \{\eta \in \mathbb{R}^n : |G^r_{j(i)}\eta| \le \hat{u}_{r(i)}, \\ i \in \mathbb{I}[1, n_u]\},\ j \in \mathbb{I}[1, s]. \tag{13}$$

Note that u_k and v_k have the forms

$$u_k = \mathcal{R}^T\eta_k,\ v_k = K^y_{\sigma_k}\bar{C}_{\sigma_k}\eta_k + K^u_{\sigma_k}\mathcal{R}^T\eta_k + K^y_{\sigma_k}\Psi_{\sigma_k}Ew_k,$$

and denote $\sigma_k = j$. The following lemma then follows directly.

Lemma 2: If $\eta \in \mathcal{S}(G^a_j, \hat{u}_a) \bigcap \mathcal{S}(G^r_j, \hat{u}_r)$, then for any $n_u \times n_u$ diagonal matrices $H^a_j > 0$ and $H^r_j > 0$ $(j \in \mathbb{I}[1, s])$, the following modified sector conditions hold:

$$\psi_a^T(u)H^a_j\left[\psi_a(u) - G^a_j\eta + \mathcal{R}^T\eta\right] \le 0,\ j \in \mathbb{I}[1, s], \tag{14}$$
$$\psi_r^T(v)H^r_j\left[\psi_r(v) - G^r_j\eta + K^y_j\bar{C}_j\eta + K^u_j\mathcal{R}^T\eta + K^y_j\Psi_jEw\right] \le 0,\ j \in \mathbb{I}[1, s]. \tag{15}$$

Remark 2: The sets $\mathcal{S}(G^a_j, \hat{u}_a)$ and $\mathcal{S}(G^r_j, \hat{u}_r)$ $(j \in \mathbb{I}[1, s])$ defined in (12) and (13) are polyhedral regions in $\mathbb{R}^n$, described respectively by the inequalities $|G^a_{j(i)}\eta| \le \hat{u}_{a(i)}$ and $|G^r_{j(i)}\eta| \le \hat{u}_{r(i)}$, $i \in \mathbb{I}[1, n_u]$. Their intersection $\mathcal{S}(G^a_j, \hat{u}_a) \bigcap \mathcal{S}(G^r_j, \hat{u}_r)$ defines the admissible state region where both sector conditions (14) and (15) hold. Alternatively, the saturation nonlinearities $\mathrm{sat}_r(v_k)$ and $\mathrm{sat}_a(u_k)$ can be represented directly via polytopic models [57], rather than using the sector conditions (14) and (15). However, such a formulation typically results in a substantially higher computational burden.

The main objective of this paper is to design the feedback input (9) such that the augmented closed-loop system (10) exhibits the following desirable properties:

1) the states are bounded for admissible η_0 and w_k;
2) the H_∞ performance requirement

$$\sum_{k=0}^{+\infty}\bar{z}_k\bar{z}_k \le \gamma\sum_{k=0}^{+\infty}w_k^Tw_k + \gamma V_0\ (\gamma > 0) \tag{16}$$

is satisfied, where V_k is the Lyapunov function; and
3) the local stability is ensured for the case $w_k \equiv 0$.

III. MAIN RESULTS

A. The control synthesis under the RR protocol

The RR protocol is a token-ring-based strategy that schedules sensor transmissions in a fixed circular order. Under the RR protocol, the function σ_k that is utilized to denote the activated node satisfies the relation $\sigma_{k+s} = \sigma_k$ [29], [58]. Without loss of generality, we can set $\sigma_k = k + 1$ for $k \in \mathbb{I}[0, s-1]$. Consequently, the activation sequence unfolds as: $\sigma_0 = 1, \sigma_1 = 2, \ldots, \sigma_{s-1} = s, \sigma_s = 1, \sigma_{s+1} = 2, \ldots$.

In this subsection, the corresponding analysis is based on the following switched Lyapunov function:

$$V_k = \eta_k^TP_{\sigma_k}\eta_k\ (P_j > 0,\ j \in \mathbb{I}[1, s]). \tag{17}$$

Let $P_{\sigma_k} = P_j$ $(j \in \mathbb{I}[1, s])$ at the time step k. Then, under the RR protocol, we have $P_{\sigma_{k+1}} = P_{j+1}$ $(P_{s+1} = P_1)$.

Theorem 1: Suppose that there exist $n \times n$ matrices $P_j > 0$, $n_u \times n_y$ matrices K^y_j, $n_u \times n_u$ matrices K^u_j, $n_u \times n$ matrices G^a_j, G^r_j, $n_u \times n_u$ diagonal matrices $\bar{H}^a_j > 0$, $\bar{H}^r_j > 0$ $(j \in \mathbb{I}[1, s])$, and any scalars $\gamma > 0$, $\nu > 0$ $(\nu \le 1/\mu)$, such that the following matrix inequalities are feasible:

$$\begin{bmatrix} -P_j & \Gamma^{12}_j & \Gamma^{13}_j & 0 & \hat{A}^T_j & \bar{F}^T \\ * & -2\bar{H}^a_j & 0 & 0 & \bar{H}^a_j\bar{B}^T & 0 \\ * & * & -2\bar{H}^r_j & \Gamma^{34}_j & \bar{H}^r_j\mathcal{R}^T & 0 \\ * & * & * & -I & \hat{D}^T_j & 0 \\ * & * & * & * & -P^{-1}_{j+1} & 0 \\ * & * & * & * & * & -\gamma I \end{bmatrix} < 0,$$

$$j \in \mathbb{I}[1,s]\ (P_{s+1}=P_1), \tag{18}$$

$$\begin{bmatrix} \nu\hat{u}^2_{a(i)} & G^a_{j(i)} \\ * & P_j \end{bmatrix} > 0,\ i \in \mathbb{I}[1,n_u],\ j \in \mathbb{I}[1,s], \tag{19}$$

$$\begin{bmatrix} \nu\hat{u}^2_{r(i)} & G^r_{j(i)} \\ * & P_j \end{bmatrix} > 0,\ i \in \mathbb{I}[1,n_u],\ j \in \mathbb{I}[1,s] \tag{20}$$

where

$$\begin{aligned}
\Gamma^{12}_j =&(G^a_j)^T - \mathcal{R},\ \Gamma^{34}_j = -K^y_j\Psi_j E,\\
\Gamma^{13}_j =&(G^r_j)^T - (K^y_j\bar{C}_j)^T - \mathcal{R}(K^u_j)^T,\\
\hat{A}_j =&\bar{A}_j + \mathcal{R}K^y_j\bar{C}_j + \mathcal{R}K^u_j\mathcal{R}^T,\\
\hat{D}_j =&\bar{D}_j + \mathcal{R}K^y_j\Psi_j E.
\end{aligned}$$

Then, 1) the states of the augmented system (10) are bounded for any η_0 satisfying $V_0 \le 1/\nu - \mu$ and any w_k satisfying (2); 2) the H_∞ performance constraint (16) is ensured; 3) the asymptotic stability of the system (10) can be guaranteed for any η_0 satisfying $V_0 \le 1/\nu$ for the case $w_k \equiv 0$ ($k \ge 0$).

Proof: Denote $H^a_j \triangleq (\bar{H}^a_j)^{-1}$ and $H^r_j \triangleq (\bar{H}^r_j)^{-1}$. Pre- and post-multiplying (18) by $\mathrm{diag}\{I, H^a_j, H^r_j, I, I, I\}$ and its transpose, respectively. Then, an application of the Schur complement yields the following matrix inequalities:

$$\begin{aligned}
&\Gamma_j + \Pi^T_j P_{j+1}\Pi_j + (1/\gamma)\tilde{F}^T\tilde{F} < 0,\\
&\quad j \in \mathbb{I}[1,s]\ \ (P_{s+1}=P_1)
\end{aligned} \tag{21}$$

where

$$\begin{aligned}
\Gamma_j =& \begin{bmatrix} -P_j & \Gamma^{12}_j H^a_j & \Gamma^{13}_j H^r_j & 0 \\ & -2H^a_j & 0 & 0 \\ & * & -2H^r_j & H^r_j\Gamma^{34}_j \\ & * & * & -I \end{bmatrix},\\
\Pi_j =&[\hat{A}_j\ \ \bar{B}\ \ \mathcal{R}\ \ \hat{D}_j],\ \tilde{F} = [\bar{F}\ \ 0\ \ 0\ \ 0].
\end{aligned}$$

Again, applying Schur complement to (19) and (20) yields

$$(G^a_{j(i)})^T G^a_{j(i)} \le \nu\hat{u}^2_{a(i)}P_j,\ i \in \mathbb{I}[1,n_u],\ j \in \mathbb{I}[1,s], \tag{22}$$

$$(G^r_{j(i)})^T G^r_{j(i)} \le \nu\hat{u}^2_{r(i)}P_j,\ i \in \mathbb{I}[1,n_u],\ j \in \mathbb{I}[1,s]. \tag{23}$$

Let $P_{\sigma_k} = P_j$ ($\mathbb{I}[1,s]$). Then, we have $P_{\sigma_{k+1}} = P_{j+1}$. Moreover, from (10), (14), (15), (17), we have

$$\begin{aligned}
&V_{k+1} - V_k + (1/\gamma)z^T_k z_k - w^T_k w_k\\
\le&\eta^T_{k+1}P_{j+1}\eta_{k+1} - \eta^T_k P_j\eta_k + (1/\gamma)z^T_k z_k\\
&- 2\psi^T_a(u_k)H^a_j\big[\psi_a(u_k) - G^a_j\eta_k + \mathcal{R}^T\eta_k\big]\\
&- 2\psi^T_r(v_k)H^r_j\big[\psi_r(v_k) - G^r_j\eta_k + K^y_j\bar{C}_j\eta_k\\
&\quad + K^u_j\mathcal{R}^T\eta_k + K^y_j\Psi_j E w_k\big] - w^T_k w_k\\
=&\zeta^T_k[\Gamma_j + \Pi^T_j P_{j+1}\Pi_j + (1/\gamma)\tilde{F}^T\tilde{F}]\zeta_k
\end{aligned} \tag{24}$$

where $\zeta_k = \mathrm{col}\{\eta_k, \psi_a(u_k), \psi_r(v_k), w_k\}$.

Combining (21) and (24), we obtain

$$V_{k+1} - V_k + (1/\gamma)z^T_k z_k - w^T_k w_k < 0. \tag{25}$$

Summing up both sides of (25) from 0 to $k-1$ yields

$$V_k + (1/\gamma)\sum_{\hat{i}=0}^{k-1} z^T_{\hat{i}} z_{\hat{i}} < \sum_{\hat{i}=0}^{k-1} w^T_{\hat{i}} w_{\hat{i}} + V_0. \tag{26}$$

Furthermore, one can see from (17), (22) and (23) that

$$\begin{aligned}
&\eta^T_k(G^a_{j(i)})^T G^a_{j(i)}\eta_k \le \nu\hat{u}^2_{a(i)}\eta^T_k P_j\eta_k\\
\le&\nu\hat{u}^2_{a(i)}V_k,\quad i \in \mathbb{I}[1,n_u],\ j \in \mathbb{I}[1,s],
\end{aligned} \tag{27}$$

$$\begin{aligned}
&\eta^T_k(G^r_{j(i)})^T G^r_{j(i)}\eta_k \le \nu\hat{u}^2_{r(i)}\eta^T_k P_j\eta_k\\
\le&\nu\hat{u}^2_{r(i)}V_k,\quad i \in \mathbb{I}[1,n_u],\ j \in \mathbb{I}[1,s].
\end{aligned} \tag{28}$$

For any initial condition η_0 satisfying $V_0 \le 1/\nu - \mu$ and any disturbance input w_k satisfying (2), it is obvious from (26) that $V_k \le 1/\nu$, $k \ge 0$. Moreover, from (27) and (28), it is seen that the constraint $\eta_k \in \mathcal{S}(G^a_j, \hat{u}_a)\bigcap\mathcal{S}(G^r_j, \hat{u}_r)$ is ensured. Also, one can obtain from (17) and (26) that

$$\lambda_m(P_{\sigma_k})\|\eta_k\|^2 \le V_k \le 1/\nu, \tag{29}$$

which means that the system states of (10) are bounded.

In (26), letting $k \to +\infty$ and noting that $V_{+\infty} \ge 0$, it is seen that the H_∞ performance constraint (16) is satisfied.

In the case of no disturbances, from (26)-(28), one can also conclude that the constraint $\eta_k \in \mathcal{S}(G^a_j, \hat{u}_a)\bigcap\mathcal{S}(G^r_j, \hat{u}_r)$ is satisfied for any η_0 satisfying $V_0 \le 1/\nu$. Meanwhile, one obtains from (25) that $V_{k+1} - V_k < 0$, which shows that the system (10) is asymptotically stable for any η_0 satisfying $V_0 \le 1/\nu$. The proof is now complete. ■

B. The control synthesis under the TOD protocol

In this subsection, we consider the control synthesis under the TOD protocol. The TOD protocol is a dynamical protocol under which the value of the function σ_k is determined by the following selection principle [29], [58]:

$$\sigma_k = \arg\max_{1\le l\le s}(y_{l,k} - \bar{y}_{l,k-1})^T Q_l (y_{l,k} - \bar{y}_{l,k-1}) \tag{30}$$

where $Q_l > 0$ ($l \in \mathbb{I}[1,s]$) are known weight matrices.

Denote $Q \triangleq \mathrm{diag}\{Q_1, Q_2, \ldots, Q_s\}$ and $\bar{Q}_l \triangleq Q\Psi_l$ ($l \in \mathbb{I}[1,s]$). The function σ_k in (30) can be rewritten as

$$\sigma_k = \arg\max_{1\le l\le s}(y_k - \bar{y}_{k-1})^T \bar{Q}_l (y_k - \bar{y}_{k-1}). \tag{31}$$

According to (31), we have the following inequality:

$$\sum_{l=1,\ l\ne\sigma_k}^{s} \lambda_{\sigma_k l}\tilde{y}^T_k Q(\Psi_{\sigma_k} - \Psi_l)\tilde{y}_k \ge 0 \tag{32}$$

where $\tilde{y}_k = y_k - \bar{y}_{k-1}$, and $\lambda_{jl} \ge 0$ ($j, l \in \mathbb{I}[1,s]$).

Furthermore, we select the Lyapunov function

$$V_k = \eta^T_k P\eta_k,\ P > 0. \tag{33}$$

Using (31) and (32), and similar to the proof of Theorem 1, the following control synthesis criterion is readily established.

Theorem 2: The conclusions of Theorem 1 are ensured under the TOD protocol if there exist $n \times n$ matrices $P > 0$, $n_u \times n_y$ matrices K^y_j, $n_u \times n_u$ matrices K^u_j, $n_u \times n$ matrices G^a_j, G^r_j, $n_u \times n_u$ diagonal matrices $\bar{H}^a_j > 0$, $\bar{H}^r_j > 0$, and any scalars $\lambda_{jl} > 0$, $\gamma > 0$, $\nu > 0$ ($\nu \le 1/\mu$) ($j, l \in \mathbb{I}[1,s]$), such that the following inequalities are feasible:

$$\begin{bmatrix} \Gamma^{11}_{jl} & \Gamma^{12}_j & \Gamma^{13}_j & \Gamma^{14}_{jl} & \hat{A}^T_j & \bar{F}^T \\ * & -2\bar{H}^a_j & 0 & 0 & \bar{H}^a_j\bar{B}^T & 0 \\ * & * & -2\bar{H}^r_j & \Gamma^{34}_j & \bar{H}^r_j\mathcal{R}^T & 0 \\ * & * & * & -I & \hat{D}^T_j & 0 \\ * & * & * & * & -P^{-1} & 0 \\ * & * & * & * & * & -\gamma I \end{bmatrix} < 0,$$

$$j,l\in\mathbb{I}[1,s],\ j\neq l, \tag{34}$$

$$\begin{bmatrix}\nu\hat{u}^2_{a(i)} & G^a_{j(i)}\\ * & P\end{bmatrix}>0,\ i\in\mathbb{I}[1,n_u],\ j\in\mathbb{I}[1,s], \tag{35}$$

$$\begin{bmatrix}\nu\hat{u}^2_{r(i)} & G^r_{j(i)}\\ * & P\end{bmatrix}>0,\ i\in\mathbb{I}[1,n_u],\ j\in\mathbb{I}[1,s] \tag{36}$$

where Γ_j^{12}, Γ_j^{13} and Γ_j^{34} are denoted in Theorem 1, and

$$\Gamma_{jl}^{11}=-P+\sum_{l=1,\ l\neq j}^{s}\lambda_{jl}\tilde{C}^TQ(\Psi_j-\Psi_l)\tilde{C},$$

$$\Gamma_{jl}^{14}=\sum_{l=1,\ l\neq j}^{s}\lambda_{jl}\tilde{C}^TQ(\Psi_j-\Psi_l)E\ (\tilde{C}=\begin{bmatrix}C & 0 & -I\end{bmatrix}),$$

$$\Gamma_{jl}^{44}=-I+\sum_{l=1,\ l\neq j}^{s}\lambda_{jl}E^TQ(\Psi_j-\Psi_l)E.$$

C. The design of the feedback gain matrices

In this subsection, we are in a position to focus on finding feedback gain matrices that ensure the guaranteed stability region and performance. As the matrix inequalities in Theorems 1 and 2 are not LMIs, rendering them unsolvable by some existing software tools, we introduce $X_j\triangleq P_j^{-1}$ $(j\in\mathbb{I}[1,s])$ as new variables. This transformation recasts the nonlinear inequalities (18) exactly into the following LMIs:

$$\begin{bmatrix}-P_j & \Gamma_j^{12} & \Gamma_j^{13} & 0 & \hat{A}_j^T & \bar{F}^T\\ * & -2\bar{H}_j^a & 0 & 0 & \bar{H}_j^a\bar{B}^T & 0\\ * & * & -2\bar{H}_j^r & \Gamma_j^{34} & \bar{H}_j^r\mathcal{R}^T & 0\\ * & * & * & -I & \hat{D}_j^T & 0\\ * & * & * & * & -X_{j+1} & 0\\ * & * & * & * & * & -\gamma I\end{bmatrix}<0,$$

$$j\in\mathbb{I}[1,s]\ (P_{s+1}=P_1,\ X_{s+1}=X_1). \tag{37}$$

However, it is worth pointing out the following equality constraints are simultaneously introduced:

$$P_jX_j=I,\ j\in\mathbb{I}[1,s]. \tag{38}$$

Similarly, defining the new variable $X\triangleq P^{-1}$, the matrix inequalities (34) can be equivalently written as follows:

$$\begin{bmatrix}\Gamma_{jl}^{11} & \Gamma_j^{12} & \Gamma_j^{13} & \Gamma_{jl}^{14} & \hat{A}_j^T & \bar{F}^T\\ * & -2\bar{H}_j^a & 0 & 0 & \bar{H}_j^a\bar{B}^T & 0\\ * & * & -2\bar{H}_j^r & \Gamma_j^{34} & \bar{H}_j^r\mathcal{R}^T & 0\\ * & * & * & -I & \hat{D}_j^T & 0\\ * & * & * & * & -X & 0\\ * & * & * & * & * & -\gamma I\end{bmatrix}<0,$$

$$j,l\in\mathbb{I}[1,s],\ j\neq l, \tag{39}$$

$$PX=I. \tag{40}$$

Note that the resultant conditions in Theorems 1 and 2 are still not strict LMIs due to the equality constraints (38) and (40). However, the non-convex problem can be addressed by employing the CCL (Cone Complementarity Linearization) algorithm [11]. To facilitate this, we introduce the LMIs

$$\begin{bmatrix}P_j & I\\ I & X_j\end{bmatrix}\geq 0,\ j\in\mathbb{I}[1,s], \tag{41}$$

$$\begin{bmatrix}P & I\\ I & X\end{bmatrix}\geq 0. \tag{42}$$

Then, the non-convex problems in Theorems 1 and 2 can be transformed into the nonlinear optimization problems:

$$\textit{Prob.1.}\ \min_{P_j,X_j,K_j^y,K_j^u,G_j^a,G_j^r,\bar{H}_j^a,\bar{H}_j^r(j\in\mathbb{I}[1,s]),\gamma,\nu}\mathrm{tr}\Big(\sum_{j=1}^{s}P_jX_j\Big),$$
$$\text{s.t. LMIs (19), (20), (37) and (41),}$$

and

$$\textit{Prob.2.}\ \min_{P,X,K_j^y,K_j^u,G_j^a,G_j^r,\bar{H}_j^a,\bar{H}_j^r,\lambda_{jl}(j,l\in\mathbb{I}[1,s]),\gamma,\nu}\mathrm{tr}(PX),$$
$$\text{s.t. LMIs (35), (36), (39) and (42).}$$

If the objective function of Prob. 1 (Prob. 2) reaches the minimum value sn (n), then the matrix inequalities in Theorem 1 (Theorem 2) are ensured to have feasible solutions. However, these optimization problems cannot be solved directly. Fortunately, as shown in [11], [12], some algorithms can be proposed to solve the problems. However, unlike the problems in [11], [12], the disturbance tolerance level μ needs to be estimated to ensure the boundedness of the system (10) and to determine the disturbance attenuation level γ. To this end, we assume $\eta_0=0$. Under this assumption, the scalar ν in (19)-(20) and (35)-(36) can be replaced by $1/\mu$. The following algorithms can then be employed to maximize μ.

Algorithm 1: Maximization of μ under the RR protocol

1) Find a feasible solution satisfying (19), (20), (37) and (41) for the given μ. Set $m=0$, $P_j^0=P_j$, $X_j^0=X_j$ $(j\in\mathbb{I}[1,s])$.
2) Solve the optimization problem
$$\min_{P_j,X_j,K_j^y,K_j^u,G_j^a,G_j^r,\bar{H}_j^a,\bar{H}_j^r(j\in\mathbb{I}[1,s]),\gamma}\mathrm{tr}\Omega_{m,s}$$
where
$$\Omega_{m,s}\triangleq\Big[\sum_{j=1}^{s}(P_jX_j^m+X_jP_j^m)\Big]$$
$$\text{s.t. LMIs (19), (20), (37) and (41).}$$
3) If the matrix inequalities (18) are feasible for the variables obtained in Step 2 and the condition
$$\Big|\mathrm{tr}\Big(\sum_{j=1}^{s}P_jX_j\Big)-sn\Big|<\delta$$
is satisfied for a sufficiently small scalar δ, then set $\mu_M=\mu$, increase μ by $\Delta\mu$, and go to Step 1.
4) If $k>N$, where N is the maximum iteration number given in advance, exit.
5) Set $m=m+1$, $P_j^m=P_j$, $X_j^m=X_j$ $(j\in\mathbb{I}[1,s])$, and return to Step 2.

For a specified scalar μ $(\leq\mu_M)$, the minimum disturbance attenuation level γ_m can be obtained by modifying Algorithms 1 and 2. These corresponding algorithms are referred to as

Algorithm 2: Maximization of μ under the TOD protocol.

1) Find a feasible solution satisfying LMIs (35), (36), (39) and (42) for a given μ. Set $m=0$, $P^0=P$, $X^0=X$.
2) Solve the optimization problem
$$\min_{P,X,K_j^y,K_j^u,G_j^a,G_j^r,\bar{H}_j^a,\bar{H}_j^r,\lambda_{jl}(j,l\in\mathbb{I}[1,s]),\gamma} \mathrm{tr}(PX^k+XP^k)$$
$$\text{s.t. LMIs } (35),(36),(39) \text{ and } (42).$$
3) If (34) is feasible for the variables obtained in Step 2 and $|\mathrm{tr}(PX)-n|<\delta$ is satisfied for a sufficiently small scalar δ, then set $\mu_M=\mu$, increase μ by $\Delta\mu$, and go to Step 1.
4) If $k>N$ (N is the maximum iteration number), exit.
5) Set $m=m+1$, $P^m=P$, $X^m=X$, and return to Step 2.

Algorithm 3 (for the RR protocol) and *Algorithm 4* (for the TOD protocol) in the paper, which are omitted here.

Next, we address the maximization of the estimated DOA. In this case, the rows and columns corresponding to w_k and z_k in (18), (34), (37), and (39) should be removed. Note that under the RR protocol, we have assumed $\sigma_0=1$. The resulting estimate of the DOA under the RR protocol can then be characterized by the ellipsoid

$$\mathscr{W}_{RR}\triangleq\{\eta_0\in\mathbb{R}^n:\eta_0^TP_1\eta_0\le 1\}. \tag{43}$$

Let $\tilde{\eta}_0\triangleq\mathrm{col}\{x_0,u_0\}$. Under the assumption that $\bar{y}_{-1}=0$, we aim to maximize the following ellipsoid:

$$\tilde{\mathscr{W}}_{RR}\triangleq\{\tilde{\eta}_0\in\mathbb{R}^{\tilde{n}}:\tilde{\eta}_0^T\tilde{P}_1\tilde{\eta}_0\le 1\} \tag{44}$$

where $\tilde{P}_1=\Upsilon P_1\Upsilon^T$ with $\Upsilon=[I_{\tilde{n}}\ \ 0_{\tilde{n}\times n_y}]$ and $\tilde{n}=n_x+n_u$.

As in [57], we can choose a reference ellipsoid

$$\mathscr{W}_0\triangleq\{\tilde{\eta}_0\in\mathbb{R}^{\tilde{n}}:\tilde{\eta}_0^TS\tilde{\eta}_0\le 1,S>0\} \tag{45}$$

such that $\alpha\mathscr{W}_0\subseteq\tilde{\mathscr{W}}_{RR}$ ($\alpha>0$), which is equivalent to

$$(1/\alpha^2)S-\tilde{P}_1\ge 0. \tag{46}$$

Remark 3: It is well known that the exact characterization of the DOA is generally impossible. Under the RR protocol with $\sigma_0=1$, the ellipsoid (43) serves as an estimate of the DOA, ensuring that any trajectory starting from it will enter the set $\cup_{j=1}^sP_j$ and eventually converge to origin. If the assumption $\sigma_0=1$ is removed, the set $\cup_{j=1}^sP_j$ itself can be taken as a DOA estimate. Furthermore, besides the set (45), the reference set may also be chosen as a polyhedron $\mathrm{co}\{x_1,x_2,\ldots,x_l\}$ [23], where "co" denotes the convex hull. Although the use of a polyhedron can potentially lead to a larger DOA estimate, it also entails a significant increase in computational burden.

By maximizing the scalar α, one can obtain the maximum ellipsoid $\tilde{\mathscr{W}}_{RR}$. The algorithm of maximizing α can be readily obtained by modifying *Algorithm 1* with the constraint (46), which is referred to as *Algorithm 5* and omitted here.

Under the TOD protocol, we will consider the ellipsoid

$$\tilde{\mathscr{W}}_{TOD}\triangleq\{\tilde{\eta}_0\in\mathbb{R}^{\tilde{n}}:\tilde{\eta}_0^T\tilde{P}\tilde{\eta}_0\le 1\}. \tag{47}$$

where $\tilde{P}=\Upsilon P\Upsilon^T$. Similarly, the maximization of the region $\tilde{\mathscr{W}}_{TOD}$ can be achieved by maximizing α of the inequality

$$(1/\alpha^2)S-\tilde{P}\ge 0. \tag{48}$$

The corresponding algorithm can be easily obtained, which is referred to as *Algorithm 6* in the subsequent part.

Remark 4: The conditions in Theorems 1 and 2 are non-convex, as they involve the inverse matrices P_j^{-1} ($j\in\mathbb{I}[1,s]$) and P^{-1}. This non-convexity persists even when $C=I$ because the incorporation of communication protocols and rate constraints prevents the elimination of matrix couplings via standard congruence transformations. Consequently, conventional linearization techniques for designing static output-feedback controllers become inapplicable [7], [18], [27].

Remark 5: Introducing the matrices X_j ($j\in\mathbb{I}[1,s]$) and X as new variables allows the matrix inequalities in Theorems 1 and 2 to be formulated as LMIs. Despite this, the resulting conditions remain non-convex due to the introduced equality constraints. Fortunately, using the idea of cone complementarity [11], [12], such non-convex feasibility problems can be converted into nonlinear minimization problems subject to LMI constraints. Subsequently, some iterative algorithms are proposed to solve the nonlinear minimization problems.

Remark 6: In Algorithms 1-6, the inner iterations are utilized to solve the nonlinear minimization problems, while the outer loops are employed to obtain the feedback gain matrices with optimized performance indices. Noting the stopping conditions in Step 3, it can be seen that these iterative algorithms cannot provide the globally optimal solutions. In fact, we can only obtain the suboptimal performance indices. Therefore, although the algorithms are always effective, some conservatism still exists because the linearized approximation potentially excludes some valid solutions. Moreover, these algorithms depend on the availability of initial feasible solutions in Step 1. If the scalars μ, γ and α are chosen appropriately, for instance, by taking μ and α sufficiently small, and γ sufficiently large, initial feasible solutions can always be obtained.

Remark 7: For the case that the actuators are only subject to amplitude constraints, we can employ the static output feedback controller $u_k=K_{\sigma_k}^y\bar{y}_k$. Denote that

$$\begin{aligned}
&\check{A}_{\sigma_k}\triangleq\begin{bmatrix}A & 0\\ \Psi_{\sigma_k}C & I-\Psi_{\sigma_k}\end{bmatrix},\ \check{D}_{\sigma_k}\triangleq\begin{bmatrix}D\\ \Psi_{\sigma_k}E\end{bmatrix},\\
&\check{C}_{\sigma_k}\triangleq[\Psi_{\sigma_k}C\ \ I-\Psi_{\sigma_k}],\ \check{B}\triangleq[B^T\ \ 0]^T,\\
&\check{F}\triangleq[F\ \ 0],\ \check{\eta}_k\triangleq\mathrm{col}\{x_k,\bar{y}_{k-1}\},
\end{aligned}$$

and choose the Lyapunov function $V_k=\check{\eta}_k^TP_{\sigma_k}\check{\eta}_k$. Then, the synthesis criterion under the RR protocol is readily obtained by deleting the LMIs (20) in Theorem 1 and modifying the matrix inequalities (18) as follows:

$$\begin{bmatrix}-P_j & \Xi_j^{12} & 0 & \Xi_j^{14} & \check{F}\\ * & -2\bar{H}_j^a & \Xi_j^{23} & \bar{H}_j^a\check{B}^T & 0\\ * & * & -I & \Xi_j^{34} & 0\\ * & * & * & -P_{j+1}^{-1} & 0\\ * & * & * & * & -\gamma I\end{bmatrix}<0,\ j\in\mathbb{I}[1,s] \tag{49}$$

where $\Xi_j^{12} = (G_j^a)^T - (K_j^y \check{C}_j)^T$, $\Xi_j^{14} = A_j^T + (K_j^y \check{C}_j)^T \check{B}^T$, $\Xi_j^{23} = -K_j^y \Psi_j E$, and $\Xi_j^{34} = \check{D}_j^T + (K_j^y \Psi_j E)^T \check{B}^T$.

Following Algorithm 1, the feedback gain matrices K_j^y ($j \in \mathbb{I}[1,s]$) can be easily obtained. For comparison with the result in [30], we assume that the gain matrices are known. Under this assumption, pre- and post-multiplying (49) by $\mathrm{diag}\{P_j^{-1}, I, I, I, I\}$ and its transpose, respectively, and defining $X_j \triangleq P_j^{-1}$, $\bar{G}_j^a \triangleq G_j^a X_j$, yields the following LMIs:

$$\begin{bmatrix} -X_j & \check{\Xi}_j^{12} & 0 & \check{\Xi}_j^{14} & X_j\check{F} \\ * & -2\bar{H}_j^a & \Xi_j^{23} & \bar{H}_j^a\check{B}^T & 0 \\ * & * & -I & \Xi_j^{34} & 0 \\ * & * & * & -X_{j+1} & 0 \\ * & * & * & * & -\gamma I \end{bmatrix} < 0,\ j \in \mathbb{I}[1,s] \tag{50}$$

where $\check{\Xi}_j^{12} = (\bar{G}_j^a)^T - (K_j^y \check{C}_j X_j)^T$ and $\check{\Xi}_j^{14} = X_j A_j^T + (K_j^y \check{C}_j X_j)^T \check{B}^T$. Similarly, it follows from (19) that

$$\begin{bmatrix} \nu\hat{u}_{a(i)}^2 & \bar{G}_{j(i)}^a \\ * & X_j \end{bmatrix} > 0,\ i \in \mathbb{I}[1,n_u],\ j \in \mathbb{I}[1,s]. \tag{51}$$

Here, the estimate of the DOA can be characterized by

$$\check{\mathscr{W}}_{RR} \triangleq \{\check{\eta}_0 \in \mathbb{R}^{n_x} : \check{\eta}_0^T \check{P}_1 \check{\eta}_0 \le 1\} \tag{52}$$

where $\check{P}_1 = \check{\Upsilon}^T P_1 \check{\Upsilon}$ with $\check{\Upsilon} = [I_{n_x} \ \ 0_{n_x \times n_y}]$.

With the matrices K_j^y ($j \in \mathbb{I}[1,s]$) assumed known, the problem of maximizing the set $\check{\mathscr{W}}_{RR}$ reduces to maximizing the scalar α subject to the LMIs (50), (51), and the condition

$$\begin{bmatrix} S/\alpha^2 & \check{\Upsilon} \\ \check{\Upsilon}^T & X_1 \end{bmatrix} \ge 0.$$

IV. Numerical examples

Example 1: Consider the system (1) with the parameters

$$A = \begin{bmatrix} 1.1 & 0.15 \\ 0.03 & 0.8 \end{bmatrix},\ B = \begin{bmatrix} 1 \\ 0.1 \end{bmatrix},\ C = I,$$
$$D = E = [0.1 \ \ 0.1]^T,\ F = [1,1].$$

Here, $q_1 = q_2 = 1$, $s = 2$, and $\hat{u}_{a(1)} = 15$, $\hat{u}_{r(1)} = 10$.

For the example, we first address the case without disturbance. Using Algorithm 5 with $\delta = 0.001$, $N = 1000$, and $S = I$ yields the maximum scalar $\alpha_M = 33.07$ and

$$\tilde{P}_1 = 10^{-3} \times \begin{bmatrix} 0.1142 & -0.0051 & 0.1820 \\ -0.0051 & 0.9068 & 0.0021 \\ 0.1820 & 0.0021 & 0.8728 \end{bmatrix},$$
$$K_1^y = [-0.2545 \ \ -0.1051],\ K_1^u = -1.2117,$$
$$K_2^y = [-0.3266 \ \ -0.1608],\ K_2^u = -1.5074.$$

Similarly, applying Algorithm 6 gives $\alpha_M = 32.97$ and

$$\tilde{P} = 10^{-3} \times \begin{bmatrix} 0.1052 & 0.0365 & 0.1781 \\ 0.0365 & 0.0992 & 0.0819 \\ 0.1781 & 0.0819 & 0.8711 \end{bmatrix},$$
$$K_1^y = [-0.2600 \ \ -0.0295],\ K_1^u = -1.1789,$$
$$K_2^y = [-0.1397 \ \ -0.0836],\ K_2^u = -0.6140.$$

Figs. 2-4 show the projections of the regions $\tilde{\mathscr{W}}_{RR}$ and $\tilde{\mathscr{W}}_{TOD}$. It can be observed that, on the whole, $\tilde{\mathscr{W}}_{TOD}$ is basically larger than $\tilde{\mathscr{W}}_{RR}$, indicating that the TOD protocol leads to a larger estimate of the DOA. In fact, for this example, the volume of the ellipsoid $\tilde{\mathscr{W}}_{TOD}$ is 1.8471×10^6, whereas the volume of $\tilde{\mathscr{W}}_{TOD}$ is 5.3933×10^5. Figs. 5-9 present the system state, the actual control input and its rate, and the selected sensor node, with the initial condition $\tilde{\eta}_0 = \mathrm{col}\{60, 15, 12\}$, which lies inside both regions $\tilde{\mathscr{W}}_{RR}$ and $\tilde{\mathscr{W}}_{TOD}$. As shown in Figs. 5 and 6, the proposed method effectively stabilizes the unstable system. Conversely, when the initial condition lies outside these regions (e.g., $\tilde{\eta}_0 = \mathrm{col}\{86, 15, 12\}$), the closed-loop stability cannot be guaranteed. Moreover, Figs. 7 and 8 reveal that the control input and its rate are saturated during the initial period, confirming the influence of actuator amplitude and rate constraints. Also, Fig. 9 illustrates that the sensors are scheduled according to a dynamic selection principle.

Next, we consider the case with disturbance. Using Algorithms 1 and 2 with $\delta = 0.001$ and $N = 1000$, the maximum disturbance tolerance levels are found to be $\mu_M = 4.68 \times 10^4$ under the RR protocol and $\mu_M = 4.37 \times 10^4$ under the TOD protocol. For the RR protocol, setting $\mu = 4 \times 10^4$ and applying Algorithm 3 yields the disturbance attenuation level $\gamma_m = 3.79$ and the following gains:

$$K_1^y = [-0.2708 \ \ -0.0727],\ K_1^u = -0.9644,$$
$$K_2^y = [-0.2294 \ \ -0.1940],\ K_2^u = -1.0828.$$

Under the TOD protocol, Algorithm 4 gives $\gamma_m = 7.20$ and

$$K_1^y = [-0.2866 \ \ 0.0089],\ K_1^u = -0.9216,$$
$$K_2^y = [-0.1459 \ \ -0.2748],\ K_2^u = -0.9947.$$

In Figs. 10 and 11, we plot the evolutions of the system states under the RR and TOD protocols, where w_k is set as

$$w_k = \begin{cases} 100,\ 0 \le k \le 3, \\ 0,\ k \ge 4. \end{cases}$$

From Figs. 10 and 11, it is seen that the control performances under the RR and TOD protocols are almost the same.

Finally, we compare the proposed method with existing results under the RR protocol. By solving the optimization problem associated in [30] with $K = [-0.5 \ \ -1]$, $\lambda = \beta = 1$, $\eta_m = \eta_M = \tau_M = 0$, $\bar{\tau}_M = 1$, and the optimized scalars $\mu = 1.36$, $\sigma = 0.47$, the resulting Lyapunov matrix is

$$P = \begin{bmatrix} 0.0008 & 0.0003 \\ 0.0003 & 0.0034 \end{bmatrix}.$$

Meanwhile, solving the optimization problem in Remark 7 of this paper with $K_1^y = K_2^y = [-0.5 \ \ -1]$ and $S = I$ yields

$$\check{P}_1 = 10^{-3} \times \begin{bmatrix} 0.0540 & 0.0195 \\ 0.0195 & 0.1247 \end{bmatrix}.$$

Moreover, using Remark 7 and performing the corresponding algorithm with $S = I$ and $\alpha = 120.51$, the following controller gains are specifically designed:

$$K_1^y = [-0.1311 \ \ 0.0035],$$
$$K_2^y = [-1.2647 \ \ -0.6141],$$

and the associated Lyapunov matrix is obtained as

$$\check{P}_1 = 10^{-4} \times \begin{bmatrix} 0.6764 & 0.0189 \\ 0.0189 & 0.6587 \end{bmatrix}.$$

Based on the above Lyapunov matrices, the areas of the corresponding DOA estimates are computed as 2.5829×10^3, 5.2551×10^4, and 6.2784×10^4, respectively. In particular, the condition established in Remark 7 yields a DOA estimate that is 20.3457 times that obtained in [30], demonstrating the potential benefit of the techniques employed in this work. Moreover, within the presented design framework, the estimated DOA is improved by 19.47% compared with the case that relies on known controller gains. Fig. 12 further illustrates the DOA estimates associated with these Lyapunov matrices.

Example 2: Consider the linearized dynamic model of the inverted pendulum system presented in [44]

$$\begin{bmatrix} \dot{\phi}_t \\ \ddot{\phi}_t \end{bmatrix} = \begin{bmatrix} 0 & 1 \\ \frac{(\mathbf{m}+\mathbf{M})\mathbf{g}}{\mathbf{M}\mathbf{l}} & 0 \end{bmatrix} \begin{bmatrix} \phi_t \\ \dot{\phi}_t \end{bmatrix} + \begin{bmatrix} 0 \\ -\frac{1}{\mathbf{M}\mathbf{l}} \end{bmatrix} \bar{u}_t.$$

where ϕ denotes the pendulum angle, $\bar{u}$ is the force applied to the cart, and the physical parameters are

$$\mathbf{m} = 0.1\text{kg}, \ \mathbf{M} = 0.1\text{kg}, \ \mathbf{l} = 0.136\text{m}, \ \mathbf{g} = 9.81\text{m/s}^2.$$

Using a sampling time of $h = 10\text{ms}$, the corresponding discretized model (see [44]) is given by

$$x_{k+1} = \begin{bmatrix} 1.0018 & 0.01 \\ 0.36 & 1.0018 \end{bmatrix} x_k + \begin{bmatrix} -0.001 \\ -0.184 \end{bmatrix} \bar{u}_k.$$

In this example, we set the output matrix as $C = I$ and choose $q_1 = q_2 = 1$, $s = 2$. The input $\bar{u}$ is subject to both amplitude and rate constraints with $\hat{u}_{a(1)} = 1$ and $\hat{u}_{r(1)} = 0.5$.

Applying Algorithm 5 with $\delta = 0.001$, $N = 2000$, and $S = I$ yields $\alpha_M = 0.419$ together with

$$\tilde{P}_1 = \begin{bmatrix} 5.4985 & 0.7413 & -0.6085 \\ 0.7413 & 1.2471 & -0.0432 \\ -0.6085 & -0.0432 & 0.2901 \end{bmatrix},$$
$$K_1^y = [3.2312 \ \ 0.7364], \ K_1^u = -1.2845,$$
$$K_2^y = [1.5041 \ \ 0.3753], \ K_2^u = -0.6465.$$

Similarly, Algorithm 6 gives $\alpha_M = 0.400$ and

$$\tilde{P} = \begin{bmatrix} 6.0116 & 0.8383 & -0.7317 \\ 0.8383 & 1.2956 & -0.0547 \\ -0.7317 & -0.0547 & 0.3464 \end{bmatrix},$$
$$K_1^y = [3.0783 \ \ 0.5695], \ K_1^u = -1.2791,$$
$$K_2^y = [1.0695 \ \ 0.2926], \ K_2^u = -0.4317.$$

In Figs. 13-16, we plot the system state, the actual control input and its rate, where $\tilde{\eta}_0 = \text{col}\{0.35, 0.10, -0.30\}$. As observed in Figs. 13 and 14, the proposed method once again demonstrates its effectiveness in stabilizing the system. Furthermore, Figs. 15 and 16 clearly illustrate that the control signals are subject to amplitude and rate constraints during the initial period, thereby highlighting the saturation characteristics inherent in the design. It is worth noting that, for this example, the volume of the ellipsoid $\tilde{\mathscr{W}}_{RR}$ is 3.5442, which is larger than the volume 3.1135 of the ellipsoid $\tilde{\mathscr{W}}_{TOD}$.

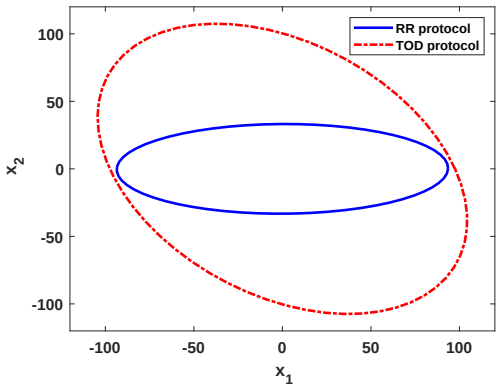

Fig. 2: The projections of $\tilde{\mathscr{W}}_{RR}$ and $\tilde{\mathscr{W}}_{TOD}$ onto x_1-x_2 plant.

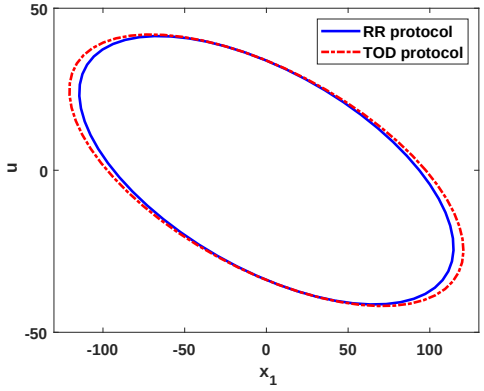

Fig. 3: The projections of $\tilde{\mathscr{W}}_{RR}$ and $\tilde{\mathscr{W}}_{TOD}$ onto x_1-u plant.

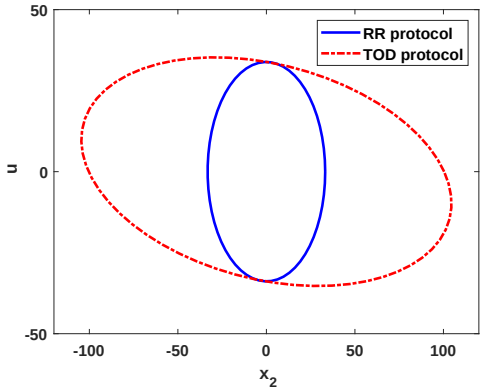

Fig. 4: The projections of $\tilde{\mathscr{W}}_{RR}$ and $\tilde{\mathscr{W}}_{TOD}$ onto x_2-u plant.

V. Conclusions

In this paper, the regional control problem have been investigated for NCSs under the RR and TOD protocols, subject to both actuator amplitude and rate constraints. Unlike prior works such as [4], [30], which have primarily focused on communication protocols, the present study has explicitly incorporated actuator rate constraints. Moreover, in contrast to [30], we have systematically designed the feedback gain matrices instead of assuming them known. Numerical results

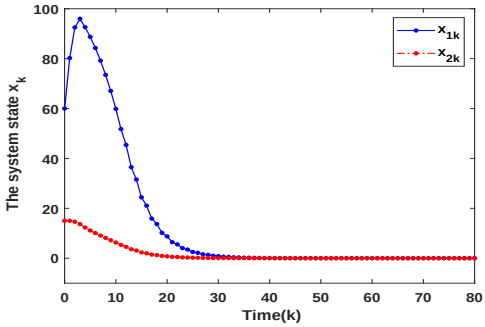

Fig. 5: The evolution of the system state (RR protocol).

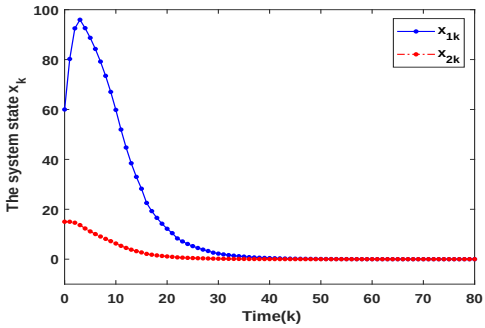

Fig. 6: The evolution of the system state (TOD protocol).

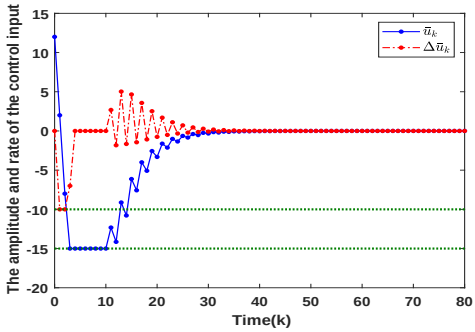

Fig. 7: The actual control input and its rate (RR protocol).

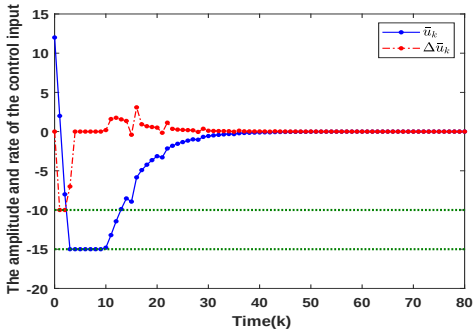

Fig. 8: The actual control input and its rate (TOD protocol).

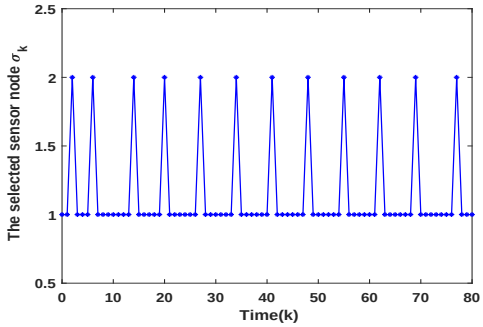

Fig. 9: The selected sensor node under the TOD protocol.

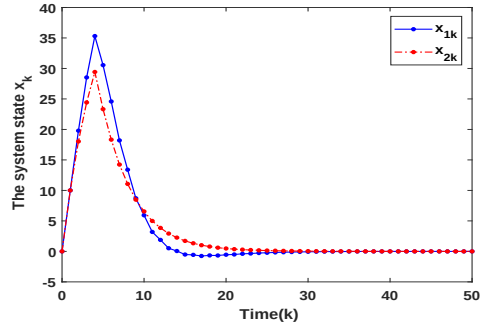

Fig. 10: The evolution of the system state (RR protocol).

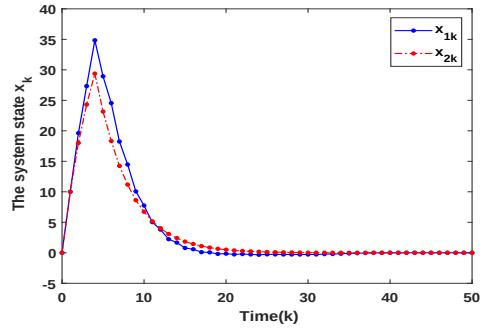

Fig. 11: The evolution of the system state (TOD protocol).

have confirmed that, even under the amplitude constraints alone, the proposed method delivers a less conservative estimate of the DOA compared with [30]. When compared to the dynamic output-feedback strategy in [4], the static feedback control developed here admits simpler implementation while maintaining satisfactory performance. It is also noteworthy that the approach in [4] does not support actuator rate constraints or the TOD protocol. Thus, the proposed findings in this paper represent a substantial supplement to the existing literature.

It is also worth noting that the communication protocols adopted in this paper are intended for node scheduling, which differs from the event-triggered scheme in [10] where the data transmission occurs only when necessary. Incorporating such an event-triggered mechanism could further reduce unnecessary transmissions and enhance the efficiency of network resource utilization, which we leave for future investigation. Additionally, the disturbances considered in this paper have been assumed to be energy-bounded, whereas in practice they

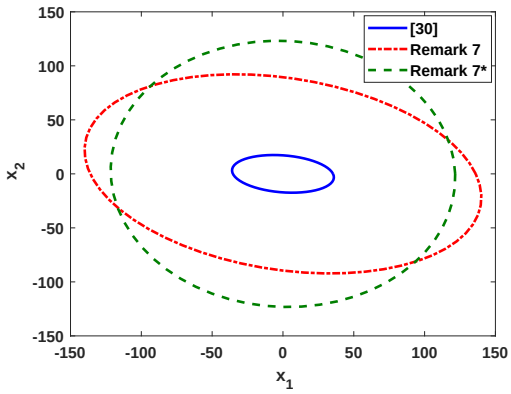

Fig. 12: The regions involving the estimate of the DOA (Remark 7: known controller gains; Remark 7*: designed controller gains).

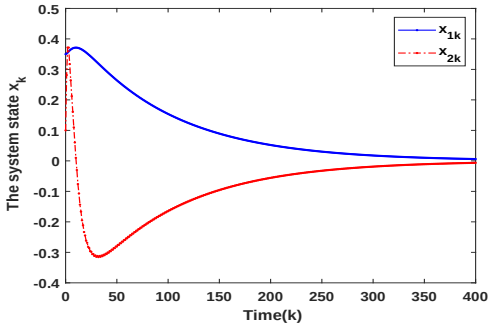

Fig. 13: The evolution of the system state (RR protocol).

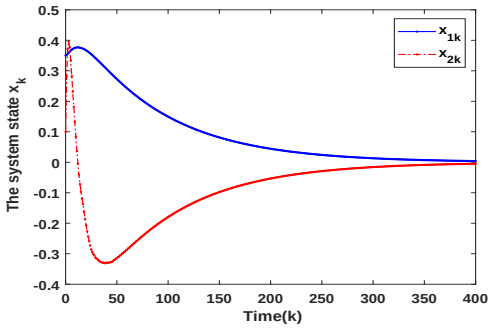

Fig. 14: The evolution of the system state (TOD protocol).

may be amplitude-bounded. Addressing the disturbance rejection problem under amplitude-bounded disturbances while ensuring DOA thus represents another important research direction [23]. Furthermore, when an accurate system model is unavailable, the data-driven control scheme offers a practical and effective alternative [10], [38], [39], which also deserves further investigation. Finally, extending the proposed framework to more general nonlinear systems, such as piecewise-affine systems [22] and T-S fuzzy systems [9], [36], [54], remains an interesting and meaningful topic for future work.

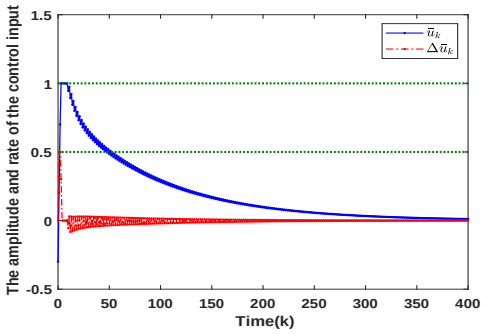

Fig. 15: The actual control input and its rate (RR protocol).

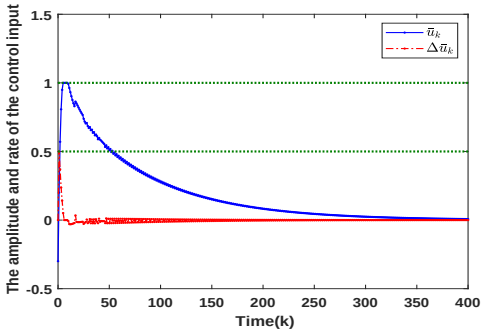

Fig. 16: The actual control input and its rate (TOD protocol).

REFERENCES

[1] R. Caballero-Águila and J. Linares-Pérez, Quadratic estimation for stochastic systems in the presence of random parameter matrices, time-correlated additive noise and deception attacks, *Journal of the Franklin Institute*, vol. 360, no. 15, pp. 11141–11164, 2023.

[2] Y. Chen and Z. Wang, Local stabilization for discrete-time systems with distributed state delay and fast-varying input delay under actuator saturations, *IEEE Transactions on Automatic Control*, vol. 66, no. 3, pp. 1337–1344, 2021.

[3] Y. Chen, Z. Wang, B. Shen, and Q.-L. Han, Local stabilization for multiple input-delay systems subject to saturating actuators: The continuous-time case, *IEEE Transactions on Automatic Control*, vol. 67, no. 6, pp. 3090–3097, 2022.

[4] Y. Chen, Z. Wang, F. E. Alsaadi, and H. Liu, Dynamic output feedback H_∞ control for state-delayed systems subject to actuator saturators under Round-Robin protocol, *International Journal of Robust and Nonlinear Control*, vol. 32, no. 3, pp. 1703–1720, 2022.

[5] Y. Chen, H. Liu, J. Hu, and H. Lin, Dynamic event-triggered regional synchronization for discrete-time delayed dynamical networks: dealing with saturating actuators, *Neurocomputing*, vol. 653, Art. no. 131179, 2025.

[6] C. de Souza, V. J. S. Leite, S. Tarbouriech, and E. B. Castelan, Event-triggered policy for dynamic output stabilization of discrete-time LPV systems under input constraints, *Systems & Control Letters*, vol. 153, art. no. 104950, 2021.

[7] D.-W. Ding and G.-H. Yang, Static output feedback for discrete-time switched linear systems under arbitrary switching, *International Journal of Control, Automation, and Systems*, vol. 8, no. 2, pp. 220–227, 2010.

[8] S. Dong and Y. Li, Adaptive fuzzy event-triggered formation control for nonholonomic multirobot systems with infinite actuator faults and range constraints, *IEEE Internet of Things Journal*, vol. 11, no. 1, pp. 1361–1373, 2024.

[9] Z. Echreshavi, M. Shasadeghi, and M. H. Asemani, H_∞ dynamic observer-based fuzzy integral sliding mode control with input magnitude and rate constraints, *Journal of the Franklin Institute*, vol. 358, no. 1, pp. 575–605, 2021.

[10] Z. Echreshavi, M. Farbood, M. Shasadeghi, and S. Mobayen, Robust event-triggered data-driven control subject to control constraints, *Soft Computing*, vol. 28, no. 23-24, pp. 13083–13096, 2024.

[11] L. El Ghaoui, F. Oustry, and M. AitRami, A cone complementarity linearization algorithm for static output-feedback and related problems, *IEEE Transactions on Automatic Control*, vol. 42, no. 8, pp. 1171–1176, 1997.

[12] H. Gao, J. Lam, C. Wang, and Y. Wang, Delay-dependent output-feedback stabilisation of discrete-time systems with time-varying state delay, *IEE Proceedings-Control Theory and Applications*, vol. 151, no. 6, pp. 691–698, 2004.

[13] Y. Gao, J. Hu, H. Yu, C. Jia, and C. Chen, Variance-constrained H_∞ state estimation for time-varying delayed neural networks with random access protocol and sensor failures, *International Journal of Network Dynamics and Intelligence*, vol. 4, no. 3, art. no. 100019, 2025.

[14] F. Garelli, P. Camocardi, and R. J. Mantz, Variable structure strategy to avoid amplitude and rate saturation in pitch control of a wind turbine, *International Journal of Hydrogen Energy*, vol. 35, no. 11, pp. 5869–5875, 2010.

[15] A. Girard, Dynamic triggering mechanisms for event-triggered control, *IEEE transactions on Automatic Control*, vol. 60, no. 7, pp. 1992–1997, 2015.

[16] J. M. Gomes da Silva Jr., S. Tarbouriech, and G. Garcia, Local stabilization of linear systems under amplitude and rate saturating actuators, *IEEE Transactions on Automatic Control*, vol. 48, no. 5, pp. 842–847, 2003.

[17] J. M. Gomes da Silva Jr., D. Limon, T. Alamo, and E. F. Camacho, Dynamic output feedback for discrete-time systems under amplitude and rate actuator constraints, *IEEE Transactions on Automatic Control*, vol. 53, no. 10, pp. 2367–2372, 2008.

[18] J. K. Goyal, S. Aggarwal, S. Ghosh, S. Kamal, and P. Dworak, L_2-based static output feedback controller design for a class of polytopic systems with actuator saturation, *International Journal of Control*, vol. 95, no. 8, pp. 2151–2163, 2022.

[19] J. P. Hespanha, P. Naghshtabrizi and Y. Xu, A survey of recent results in networked control systems, *Proceedings of the IEEE*, vol. 95, no. 1, pp. 138–162, 2007.

[20] F. Jin, L. Ma, C. Zhao and Q. Liu, State estimation in networked control systems with a real-time transport protocol, *Systems Science & Control Engineering*, vol. 12, no. 1, art. no. 2347885, 2024.

[21] R. A. Hess, and S. A. Snell, Flight control system design with rate saturating actuators, *Journal of Guidance, Control, and Dynamics*, vol. 20, no. 1, pp. 90–96, 1997.

[22] W. Hu, X. Lou, Y. Liu, and Q. Zhu, A hybrid control approach for discrete-time piecewise-affine systems with actuator saturation, *International Journal of Systems Science*, vol. 56, no. 14, pp. 3498–3511, 2025.

[23] T. Hu, Z. Lin, and B. M. Chen, Analysis and design for discrete-time linear systems subject to actuator saturation, *Systems* & *Control Letters*, vol. 45, no. 2, pp. 97–112, 2002.

[24] C. Huang, D. Yue, X. Xie, and J. Xie, Anti-windup load frequency controller design for multi-area power system with generation rate constraint, *Energies*, vol. 9, no. 5, art. no. 330, 2016.

[25] X. Jin, J. Qin, Y. Shi, and W.-X. Zheng, Auxiliary fault tolerant control with actuator amplitude saturation and limited rate, *IEEE Transactions on Systems, Man, and Cybernetics: Systems*, vol. 48, no. 10, pp. 1816–1825, 2018.

[26] C. Li, Y. Liu, M. Gao and L. Sheng, Fault-tolerant formation consensus control for time-varying multi-agent systems with stochastic communication protocol, *International Journal of Network Dynamics and Intelligence*, vol. 3, no. 1, art. no. 100004, 2024.

[27] Y.-F. Li, Design of H_∞ static output feedback control for discrete-time systems with limited actuator, *Asian Journal of Control*, vol. 17, no. 1, pp. 284–296, 2015.

[28] Y.-H. Lim, and H.-S. Ahn, Decentralized control of nonlinear interconnected systems under both amplitude and rate saturations, *Automatica*, vol. 49, no. 8, pp. 2551–2555, 2013.

[29] K. Liu, E. Fridman, and L. Hetel, Networked control systems in the presence of scheduling protocols and communication delays, *SIAM Journal on Control and optimization*, vol. 53, no. 4, pp. 1768–1788, 2015.

[30] K. Liu and E. Fridman, Discrete-time network-based control under scheduling and actuator constraints, *International Journal of Robust and Nonlinear Control*, vol. 25, no. 12, pp. 1816–1830, 2015.

[31] S. Liu, L. Wang, Y. Zhang, Y.-A. Wang and H. Dong, Recursive filtering of networked systems with communication protocol scheduling: a survey, *International Journal of Systems Science*, vol. 56, no. 11, pp. 2499–2516, 2025.

[32] L. G. Moreira, L. B. Groff, and J. M. Gomes da Silva Jr., Event-triggered state-feedback control for continuous-time plants subject to input saturation, *Journal of Control, Automation and Electrical Systems*, vol. 27, no. 5, pp. 473–484, 2016.

[33] L. A. L. Oliveira, M. V. C. Barbosa, L. F. P. Silva, and V. J. S. Leite, Exponential stabilization of LPV systems under magnitude and rate saturating actuators, *IEEE Control Systems Letters*, vol. 6, pp. 1418–1423, 2022.

[34] A. H. K. Palmeira, J. M. Gomes da Silva Jr., S. Tarbouriech, and I. M. F. Ghiggi, Sampled-data control under magnitude and rate saturating actuators, *International Journal of Robust and Nonlinear Control*, vol. 26, no. 15, pp. 3232–3252, 2016.

[35] C. Peng and F. Li, A survey on recent advances in event-triggered communication and control, *Information Sciences*, vol. 457-458, pp. 113–125, 2018.

[36] W. Qian, Y. Wu, and B. Shen, Novel adaptive memory event-triggered-based fuzzy robust control for nonlinear networked systems via the differential evolution algorithm, *IEEE/CAA Journal of Automatica Sinica*, vol. 11, no. 8, pp. 1836–1848, 2024.

[37] W. Qian, Y. Wu, and J. Yang, Event-driven reduced-order fault detection filter design for nonlinear systems with complex communication channel, *IEEE Transactions on Fuzzy Systems*, vol. 31, no. 1, pp. 281–293, 2024.

[38] H. Shen, C. Peng, H. Yan, and S. Xu, Data-driven near optimization for fast sampling singularly perturbed systems, *IEEE Transactions on Automatic Control*, vol. 69, no. 7, pp. 4689–4694, 2024.

[39] H. Shen, J. Wu, J. Wang, and Z. Wu, Adversarial dynamic games for Markov jump systems: A policy iteration Q-learning method, *Automatica*, vol. 183, art. no. 112591, 2026.

[40] S. Tarbouriech, G. Garcia, J.-M. Gomes da Silva Jr., and I. Queinnec, *Stability and Stabilization of Linear Systems with Saturating Actuators*, Springer-Verlag, London, 2011.

[41] W. Wang and M. Wang, Adaptive neural event-triggered output-feedback optimal tracking control for discrete-time pure-feedback nonlinear systems, *International Journal of Network Dynamics and Intelligence*, vol. 3, no. 2, art. no. 100010, 2024.

[42] Y. Wang, J. Wang, H. Shen, and J. H. Park, Fuzzy-model-based H_∞ reduced-order filtering for semi-markov iump nonlinear networked systems under weighted try-once-discard protocol, *IEEE Internet of Things Journal*, vol. 12, no. 20, pp. 41891–41903, 2025.

[43] X. Wang, D. Ding, H. Dong, and X.-M. Zhang, Neural-network-based control for discrete-time nonlinear systems with input saturation under stochastic communication protocol, *IEEE/CAA Journal of Automatica Sinica*, vol. 8, no. 4, pp. 766–778, 2021.

[44] W. Wu, S. Reimann, and S. Liu, Event-triggered control for linear systems subject to actuator saturation, In *Proceedings of the 19th World Congress (IFAC)*, Cape Town, South Africa, 2014, pp. 9492–9497.

[45] Y. Wu, Y. Niu and Y. Yang, Security sliding mode control for T-S fuzzy systems under attack probability-dependent dynamic round-robin protocol, *International Journal of Systems Science*, vol. 55, no. 5, pp. 926–940, 2024.

[46] Z. Wu, J. Yuan, D. Li, Y. Xue, and Y. Chen, The influence of rate limit on proportional-integral controller for first-order plus time-delay systems, *ISA Transactions*, vol. 105, pp. 157–173, 2020.

[47] H. Yang, Y. Xia Y, H. Yuan, and J. Yan. Quantized stabilization of networked control systems with actuator saturation, *International Journal of Robust and Nonlinear Control*, vol. 26, no. 16, pp. 3595–3610, 2016.

[48] Y. Yu, Y. Yuan, and H. Liu, Backstepping control for a class of nonlinear discrete-time systems subject to multisource disturbances and actuator saturation, *IEEE Transactions on Cybernetics*, vol. 52, no. 10, pp. 10924–10936, 2022.

[49] J. Zhang, C. Peng, X. Xie and D. Yue, Output feedback stabilization of networked control systems under a stochastic scheduling protocol, *IEEE Transactions on Cybernetics*, vol. 50, no. 6, pp. 2851–2860, 2020.

[50] K. Zhang, B. Zhou, and H. Jiang, Parametric Lyapunov equation based event-triggered and self-triggered control of input constrained linear systems, *International Journal of Robust and Nonlinear Control*, vol. 30, no. 6, pp. 6606–6626, 2020.

[51] H. Zhang and Z. Xiang, Finite-time robust adaptive simultaneous stabilisation of nonlinear time-delay systems with actuator saturation, *International Journal of Systems Science*, vol. 55, no. 1, pp. 49–67, 2024.

[52] L. Zhang, H. Gao, and O. Kaynak, Network-induced constraints in networked control systems-A survey, *IEEE Transactions on Industrial Informatics*, vol. 9, no. 1, pp. 403–416, 2013.

[53] R. Zhang, H. Liu, Y. Liu, and H. Tan, Dynamic event-triggered state estimation for discrete-time delayed switched neural networks with con-

strained bit rate, *Systems Science & Control Engineering*, vol. 12, no. 1, art. no. 2334304, 2024.
[54] T. Zhang, G. Feng, H. Liu, and J. Lu, Piecewise fuzzy anti-windup dynamic output feedback control of nonlinear processes with amplitude and rate actuator saturations, *IEEE Transactions on Fuzzy Systems*, vol. 17, no. 2, pp. 253–264, 2009.
[55] C. Zheng, H. Fu, J. Bai, X. Meng and Y. Chen, FlexRay protocol based distributed nonfragile dissipative filtering of state-saturated switched stochastic systems, *International Journal of Systems Science*, vol. 55, no. 4, pp. 714–727, 2024.
[56] B. Zhou, Z. Lin, and G. Duan, A parametric Lyapunov equation approach to the design of low gain feedback, *IEEE Transactions on Automatic Control*, vol. 53, no. 6, pp. 1548–1554, 2008.
[57] B. Zhou, Analysis and design of discrete-time linear systems with nested actuator saturations, *Systems & control letters*, vol. 62, no. 10, pp. 871–879, 2013.
[58] L. Zou, Z. Wang, and H. Gao, Set-membership filtering for time-varying systems with mixed time-delays under Round-Robin and Weighted Try-Once-Discard protocols, *Automatica*, vol. 74, 341–348, 2016.

Yonggang Chen received his B.Sc. and M.Sc. degrees in Mathematics from Henan Normal University, Xinxiang, China, in 2003 and 2006, respectively. He received his Ph.D. degree in Control Theory and Control Engineering from Southeast University, Nanjing, China, in 2013. From 2016 to 2017, he was a Visiting Scholar with the Department of Computer Science, Brunel University London, London, U.K. From 2006 to 2025, he served as a lecturer, associate professor, and professor in Henan Institute of Science and Technology, Xinxiang, China. He is currently a professor with the School of Mathematics and Statistics, Xinyang Normal University, Xinyang, China. His research interests include constrained control, networked control, time-delay systems and so on.

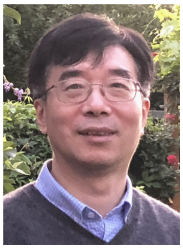

Zidong Wang (Fellow, IEEE) received the B.Sc. degree in mathematics in 1986 from Suzhou University, Suzhou, China, the M.Sc. degree in applied mathematics and the Ph.D. degree in electrical engineering both from Nanjing University of Science and Technology, Nanjing, China, in 1990 and 1994, respectively.

He is currently Professor of Dynamical Systems and Computing in the Department of Computer Science, Brunel University London, U.K. From 1990 to 2002, he held teaching and research appointments in universities in China, Germany and the UK. Prof. Wang's research interests include dynamical systems, signal processing, bioinformatics, control theory and applications. He has published a number of papers in international journals. He is a holder of the Alexander von Humboldt Research Fellowship of Germany, the JSPS Research Fellowship of Japan, William Mong Visiting Research Fellowship of Hong Kong.

Prof. Wang serves (or has served) as the Editor-in-Chief for *International Journal of Systems Science*, the Editor-in-Chief for *Neurocomputing*, the Editor-in-Chief for *Systems Science & Control Engineering*, and an Associate Editor for 12 international journals, including IEEE TRANSACTIONS ON AUTOMATIC CONTROL, IEEE TRANSACTIONS ON CONTROL SYSTEMS TECHNOLOGY, IEEE TRANSACTIONS ON NEURAL NETWORKS, IEEE TRANSACTIONS ON SIGNAL PROCESSING, and IEEE TRANSACTIONS ON SYSTEMS, MAN, AND CYBERNETICS–PART C. He is a Member of the Academia Europaea, a Member of the European Academy of Sciences and Arts, an Academician of the International Academy for Systems and Cybernetic Sciences, a Fellow of the IEEE, a Fellow of the Royal Statistical Society, and a member of program committee for many international conferences.

Juan Wang received the B.Sc. degree in Mathematics from Xinyang Normal University, Xinyang, China, in 2003, the M.Sc. degree in Applied Mathematics from Zhengzhou University, Zhengzhou, China, in 2009, and the Ph.D. degree in Systems Engineering from Beijing Institute of Information and Control, Beijing, China, in 2012. She is currently a professor with the School of Mathematics and Statistics, Xinyang Normal University, Xinyang, China. Since 2022, she has served as Vice President of Xinyang Normal University. Her research interests include systems analysis and control, biomathematics, and related areas.

Lan Lan received the B.Sc. degree in Mathematics from Henan Institute of Science and Technology, Xinxiang, China, in 2016, and the M.Sc. degree in Applied Mathematics and the Ph.D. degree in Systems Science from University of Shanghai for Science and Technology, Shanghai, China, in 2019 and 2025, respectively. She is currently a lecturer with the School of Mathematics and Statistics, Xinyang Normal University, Xinyang, China. Her research interests are multisensor information fusion, distributed filtering, and networked control systems.